# Three-Dimensional Trajectory Analysis of Two Drop Sizing Instruments: PMS* OAP and PMS* FSSP

HILLYER G. NORMENT

*Atmospheric Science Associates, Concord, Massachusetts*

(Manuscript received 30 October 1987, in final form 21 March 1988)

ABSTRACT

Flow-induced distortions of water drop flux and speed are predicted by three-dimensional calculations. The instruments are studied in isolation and mounted under the wing of a DeHavilland Twin Otter airplane. Several free stream air speeds and angles of attack of 0° and 4° are studied for drop diameters ranging from 2 to 1000 μm.

For the PMS Optical Array Probe (OAP) in isolation and under the Twin Otter wing with the airplane at 0° angle of attack, distortions of practical consequence are not found. At 4° airplane angle of attack, 17% undermeasurement of both flux and speed is predicted for cloud-size droplets.

The PMS Forward Scattering Spectrometer Probe (FSSP) presents greater flow obstruction than the OAP, and requires in addition that air and drops traverse the measurement tube. As expected, larger flow-induced effects are predicted under all circumstances than for the OAP. For the FSSP in isolation and mounted on the Twin Otter at 0° angle of attack, both speed and flux are predicted to be undermeasured by about 10% for cloud-size droplets. At 4° airplane angle of attack, 24% undermeasurement of both flux and speed is predicted for cloud-size droplets.

For the wing-mounted instruments we find that a large part of the flow-induced effects (approximately half) is caused by the instruments themselves. This shows that it is not always justified to assume that instrument-induced flow effects are insignificant compared with aircraft-induced effects.

## 1. Introduction

NASA Lewis Research Center has instrumented a DeHavilland DHC6 Twin Otter airplane for use in icing research. Considered here are a PMS Optical Array Probe (OAP) (Knollenberg 1970, 1976) and a PMS Forward Scattering Spectrometer Probe (FSSP) (Knollenberg 1976), both mounted under the wing as shown in Fig. 1. These instruments sense and size water drops and other hydrometeors. As is well known (Norment 1976, 1985a), flow perturbations caused by passage of the airplane can seriously distort the measurements. Hydrometeor trajectory calculations (Norment 1985b) provide the only practical means available for predicting these effects.

The objectives of this study were to predict water drop flux and speed distortions caused by flow about 1) the isolated instruments; and 2) complete assemblies of the instruments, their mounts and the Twin Otter airplane. Results were compared with similar results obtained by the Canadian National Aeronautical Establishment for their similarly instrumented Twin Otter (Drummond and MacPherson 1985). Similar studies of other instruments on the Twin Otter are reported elsewhere (Shaw et al. 1986).

Only effects of flow perturbations on drop trajectories were considered. Errors and biases caused by optical problems or other workings of the instruments were not addressed.

## 2. The instruments and airplane

The OAP (Fig. 2) consists of a cylindrical canister with hemispherical ends, one of which supports a pair of probe arms. A laser beam passes between the probe arms, and hydrometeors that pass through the beam are sensed and sized. Two-dimensional images of the hydrometeors are recorded by a linear array of sensors. To obtain undistorted images, the transit speeds of the hydrometeors through the beam must be known. The particle diameter range capability is approximately 75–2000 μm.

The FSSP consists of a canister, identical in size and shape with that of the OAP, and a pair of arms that support a tube (Fig. 3). Hydrometeors that pass through this measurement tube intersect a laser beam and are sized using Mie theory. Particle diameter range capability is approximately 2–100 μm.

Paneled descriptions of the instruments shown in Figs. 2 and 3 are suitable for use by the flow codes. However, since structural details of portions of the instruments located well aft of the measurement volumes

* Particle Measuring Systems, Inc., Boulder, Colorado.

*Corresponding author address:* Dr. Hillyer G. Norment, Atmospheric Science Associates, 186 Peter Spring Road, Concord, MA 01742.

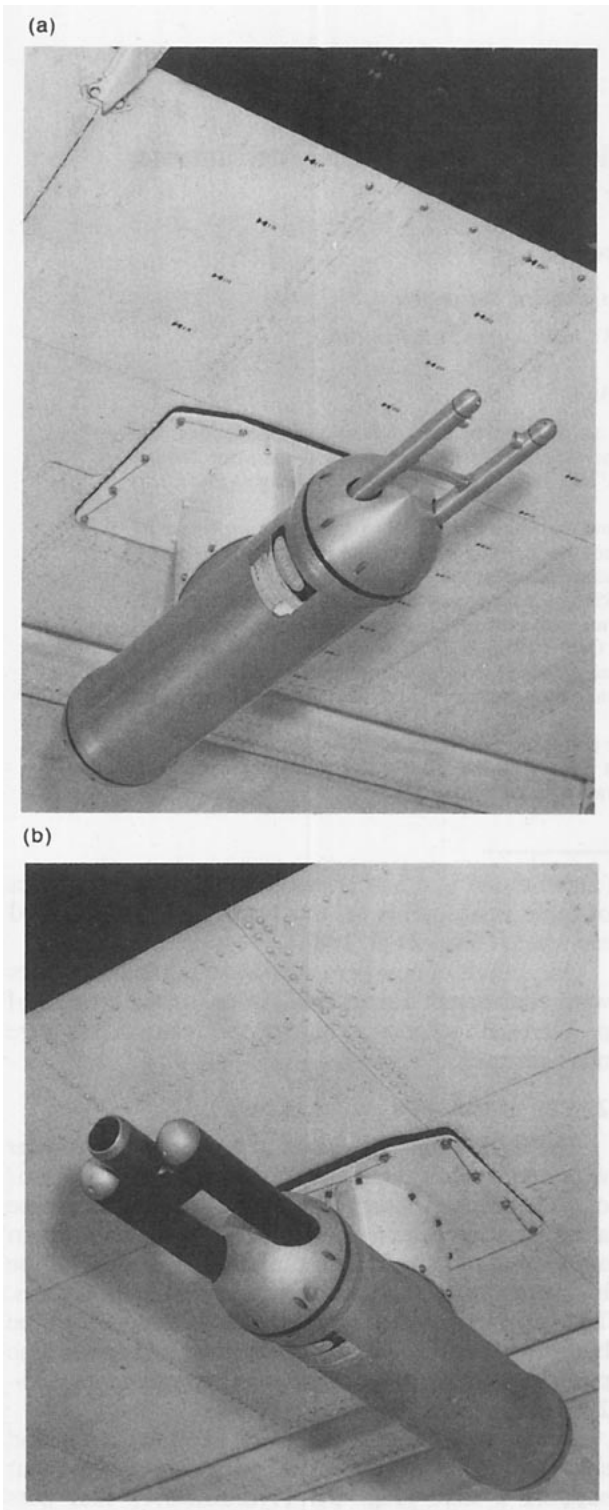


FIG. 1. PMS instruments mounted under the Twin Otter wing. (a) PMS OAP; (b) PMS FSSP.

contribute little of significance to the flow up to the measurement volumes, slightly abbreviated versions of the aft ends of the canisters were actually used.

Figure 4 shows the paneled description of the Twin Otter airplane. A crudely resolved version of the fuselage is sufficient, since both instruments are mounted toward the wing tip. The engine nacelle is not included, because comparison of concentration factor calculation results for the OAP with and without the nacelle shows an insignificant nacelle contribution. Figure 5 shows the instruments mounted under the Twin Otter wing, along with their mounting plates and pylons.

## 3. Calculation methods

Air flow about the exterior of a three-dimensional body of arbitrary shape is calculated by a modified version of a first order panel code developed by Hess (1972). Effects on the flow of wing-lift vorticity are included. The body surface must be approximated by contiguous, plane, quadrilateral panels as illustrated by Figs. 2–5. Details of the method are given by Hess (1972) and Norment (1985b), and applications are discussed by Norment (1976, 1985a). For the types of exterior flows required for this study, accuracy has been found to be adequate (Hess 1972; Norment and Zalosh 1974).

While the first order code can accommodate flow in and out of an orifice provided that flux through the orifice is specified a priori, a second order code is required to predict interior flow, such as that through the FSSP measurement tube. Since a three-dimensional, second order code was not available, an axisymmetric, second order code (Hess and Martin 1974; Friedman 1974) was used to estimate flow through the FSSP measurement tube. For the canister-measurement tube combination (without the support arms), it was calculated that a flux of 95.9% of freestream, which is independent of angle of attack, passed through the tube. To estimate the effect of the support arms on the flow, a three-dimensional calculation for the canister-support arms combination (with the measurement tube omitted) and a calculation for the canister alone were made. The difference in flow between these calculations at the intake orifice is 3.9% of freestream, which is also independent of angle of attack. Therefore, the net flux into the orifice is approximately 92% of the freestream flux.

The three-dimensional, first order code requires that orifices be paneled in the same manner as are impervious surfaces, the flux through each panel being specified by input. Figure 3 shows the paneling used for the FSSP measuring tube: each orifice is represented by twenty-one panels. For the FSSP in isolation, and when mounted under the Twin Otter wing with the airplane at 0° angle of attack, the orifice flux specification was taken to be 92% of freestream as discussed above. With the airplane at 4° angle of attack without the instrument, calculation shows an air flux of 89% of freestream at the location of the FSSP orifice (owing to partial stagnation under the wing). Accordingly, with the airplane at 4° angle of attack, flux through each

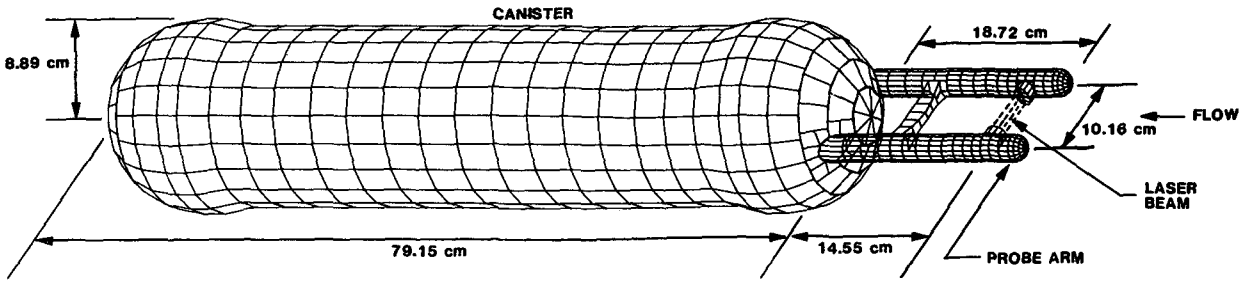


FIG. 2. Detailed digital description of the PMS OAP suitable for use by the three-dimensional flow code. Dimensional data, labeling and laser beam path are added to a computer plot.

orifice panel was taken to be 82% (92 × 0.89) of freestream.

Drop trajectories from the unperturbed freestream to the instruments are calculated by numerical integration of the drop equations of motion, including gravity. Experimental drag data for water drops (Gunn and Kinser 1949) are used for large values of drop Reynolds number, while sphere drag data (Davies 1945) are used for small Reynolds numbers. Air velocities are provided by the flow codes as needed. Details and discussions of accuracy, which is quite adequate, are given elsewhere (Norment 1985b; Norment and Zalosh 1974).

To estimate drop flux distortions seen by the instruments, a quantity called concentration factor or $C_F$, defined as

$$C_F = \frac{\text{water drop flux at the instrument sampling volume}}{\text{water drop flux in the freestream}} \quad (1)$$

is calculated. For drops of a particular size, $C_F$ is determined by computing a tube of trajectories, a flux tube, from the unperturbed freestream to the instrument sampling volume. The flux tube is defined by six trajectories that intersect the target plane at approxi-

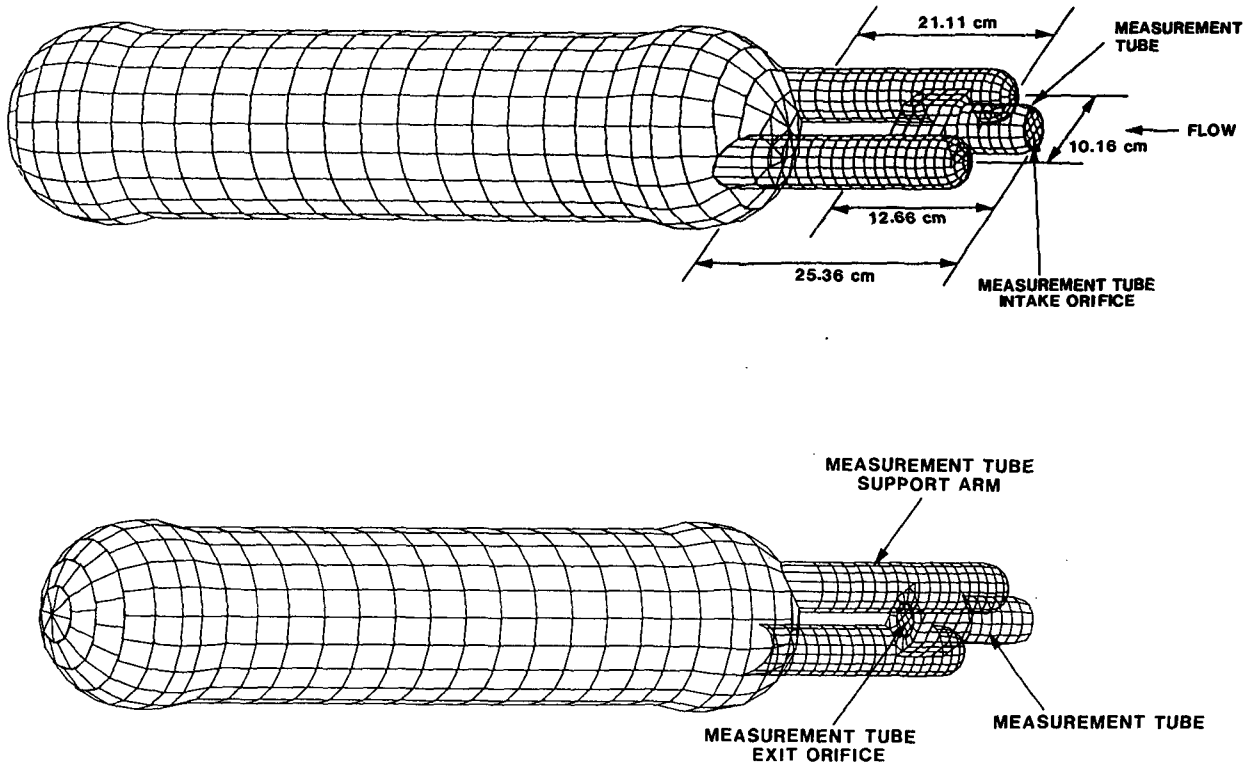


FIG. 3. Detailed digital description of the PMS FSSP suitable for use by the three-dimensional flow code. Dimensional data and labeling are added to a computer plot.

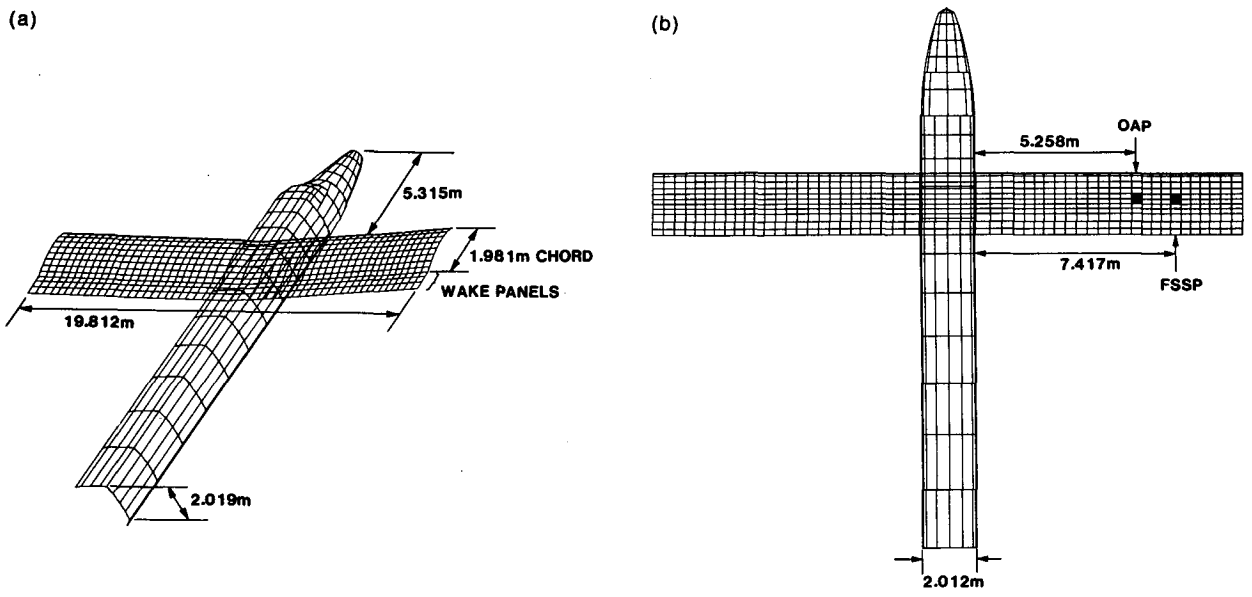


FIG. 4. Detailed digital description of the Twin Otter used for this study. Panels covered by the instrument mount plates are blackened. Dimensional data and labeling are added to a computer plot. (a) Perspective view; (b) view of the underside.

mately the corners of a small regular hexagon with its center at the center of the sampling volume. An iterative procedure is used to ensure that each trajectory end point lies within a (preset) tolerance distance of its target point. Since mass transfer rate through the tube is constant at all cross sections, it is easily shown that $C_F = A/A_t$, where $A$ and $A_t$ are flux tube cross section areas in the initial and target planes.

For the OAP, the flux tube center in the target plane is at the center of the laser beam, and the boundary target points lie on a circle with radius approximately that of the laser beam. For the FSSP, the target plane is constrained to be parallel to the plane of the measurement tube intake orifice and to lie a small distance (0.127 cm) upstream of it. The center of the flux tube in the target plane lies on the axis that passes through the center of the measurement tube. Two radii for the flux tube boundary circle in the target plane are used for the FSSP: 1) a radius slightly less (0.02 cm less) than the measurement tube inside radius (1.67 cm); and 2) a radius one-half of the measurement tube inside radius. The coarser tubes are used to assess the overall collection efficiency of the measurement tube, while the finer tubes are used to assess the measurement efficiency for those drops that are more likely to be accurately sensed and sized by the instrument.

Trajectories of large drops are initiated at a distance of at least 20.2 m (10 fuselage diameters) upstream of the target planes. This distance is not always large enough for small drops, particularly for the wing-mounted instruments at 4° angle of attack, so this distance is doubled for drops with diameters 20 $\mu$m and less.

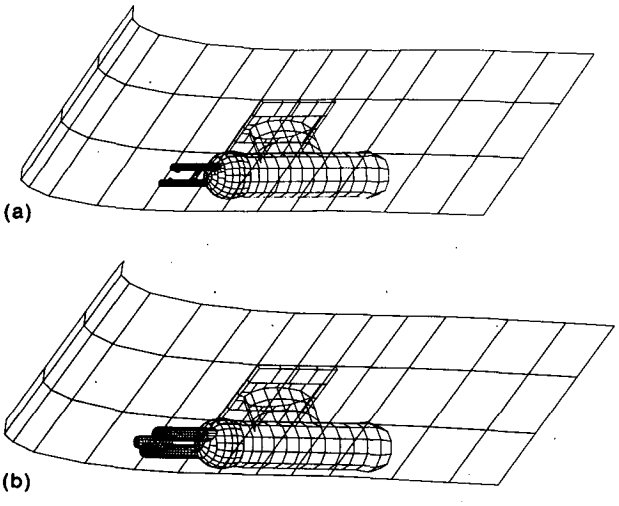


FIG. 5. Computer plots of the wing-mounted instruments including short segments of the wing. Only the underside of the wing surface is plotted to avoid confusion of overlapping lines. (a) PMS OAP; (b) PMS FSSP.

## 4. Flow fields

Figure 6 shows the flow field for the OAP mounted under the Twin Otter wing with the airplane at 0° angle of attack.[1] The instrument axis makes an angle of 5° with the wing chord plane, forward end down. How-

[1] Airplane angle of attack is the angle between the fuselage axis and the freestream vector. This is different from angle of attack for the isolated instrument, where the angle is relative to the instrument axis.

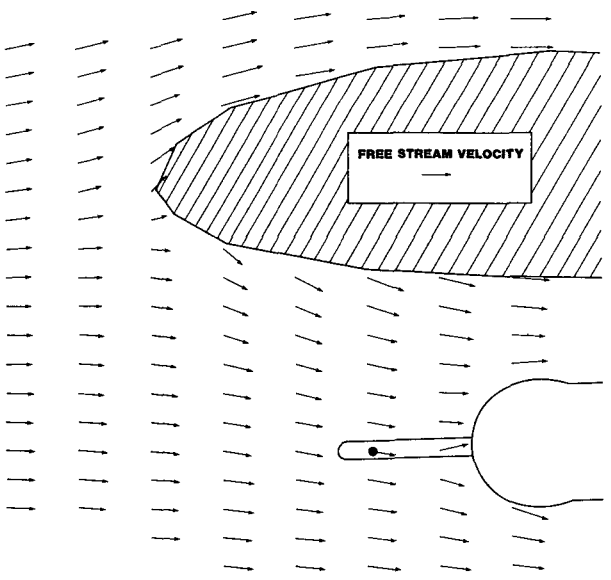


FIG. 6. Flow field in the vertical plane normal to the OAP laser beam and through its center (●). The airplane fuselage axis is at 0° angle of attack to the freestream flow.

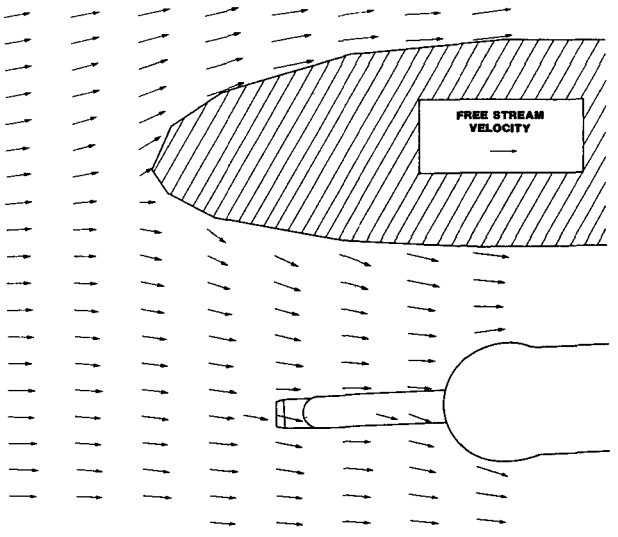


FIG. 7. Flow field in the vertical plane parallel with the airplane fuselage axis and through the center point of the FSSP measurement tube intake orifice. The airplane fuselage axis is at 0° angle of attack to the freestream flow.

ever, as mounted on the fuselage, the wing chord plane is tilted upward by 2.5° relative to the fuselage axis, so that the instrument axis has a net downward tilt of 2.5° relative to the fuselage axis and the freestream vector. (For 4° airplane angle of attack, the instrument axis makes a net 1.5° angle, forward end up, with respect to the freestream vector.) The center of the laser beam is approximately 25 cm from the wing surface. Flow vectors at the center of the laser beam have the properties shown in Table 1.

Figure 7 shows the flow field for the wing-mounted FSSP with the airplane at 0° angle of attack. Net instrument axis angles relative to the freestream vector are the same as for the OAP. The center of the measurement tube intake orifice is approximately 27 cm from the wing surface. Flow vectors at the center of the orifice have the properties shown in Table 2.

## 5. Flight conditions

Since potential flow is calculated, the flow fields are independent of atmospheric properties and air speed, but trajectory results are weakly dependent on these conditions. Atmospheric properties are those at 2.13 km (7 kft) altitude in the U.S. Standard Atmosphere (NOAA 1976). Specifically, air density is 0.993 kg $m^{-3}$ and temperature is 274.3°K. All calculations are done for two air speeds: 49 and 129 m $s^{-1}$ (95 and 250 kts) for the isolated instruments, and 49 and 67 m $s^{-1}$ (95 and 130 kts) for the mounted instruments; and all calculations are done for two angles of attack: 0° and 4°.[2]

TABLE 1. Properties of flow vectors at the center of the OAP laser beam.

| Airplane angle of attack | Magnitude relative to freestream | Angle relative to horizontal plane[a] | Angle relative to the airplane symmetry plane[b] |
|---|---|---|---|
| 0° | 96.4% | −9.2° | 1.1° |
| 4° | 83.1% | −8.9° | 1.8° |

[a] The horizontal plane is normal to the gravity vector.
[b] These angles are such as to tilt the vectors to the outboard direction.

## 6. Trajectory results

### a. General considerations

We are interested in two quantities: concentration factor and drop speed ratio. Concentration factor is unity for undistorted water drop flux at an instrument measurement volume. Drop speed ratio is the ratio of drop speed to freestream air speed at either the center of the laser beam for the OAP or into the center of the measurement tube orifice for the FSSP. This quantity is particularly important for the OAP, because it is needed to produce undistorted hydrometeor images. While it is common practice to assume that drop transit speed through the beam is the same as airplane air speed, we see below that it actually varies with instrument, drop diameter and angle of attack.

In interpreting trajectory data it is important to understand the following generalities:

[2] Though air speed and angle of attack are treated independently here, they are actually related through the lift coefficient as discussed by Drummond (1984) and Drummond and MacPherson (1984).

TABLE 2. Properties of flow vectors at the center of the FSSP orifice.

| Airplane angle of attack | Magnitude relative to freestream | Angle relative to horizontal plane[a] | Angle relative to the airplane symmetry plane[b] |
|---|---|---|---|
| 0° | 89.9% | −12.7° | 2.0° |
| 4° | 76.7% | −9.7° | 3.1° |

[a] The horizontal plane is normal to the gravity vector.
[b] These angles are such as to tilt the vectors to the outboard direction.

1. Large drops, which have high inertia, tend to ignore local flow perturbations, with the result that the large-drop tails of plots of concentration factor or speed ratio vs. drop diameter approach unity.
2. Very small drops, which have low inertia, tend to closely follow the air flow, with the result that the small-drop tails of plots of concentration factor vs. drop diameter show effects of flow divergence ($C_F < 1$) or convergence ($C_F > 1$). Drop speed ratio asymptotically approaches that of the air.
3. Intermediate size drops tend to show less predictable effects. For example, plots of concentration factor or speed ratio vs. drop diameter may show maxima or minima, sometimes sharply peaked, depending on geometry, angle of attack, and sometimes air speed.

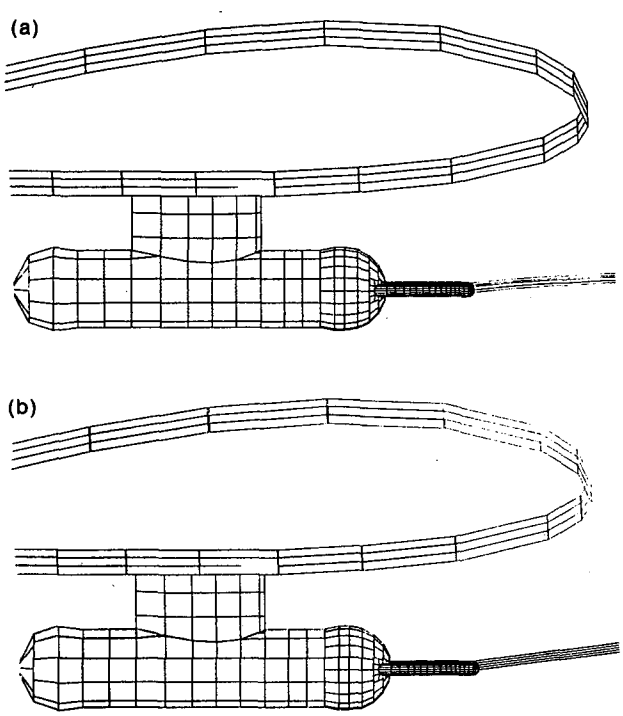


FIG. 8. Water drop flux tubes to the OAP. Airplane angle of attack is 0°, and freestream airspeed is 49 m s$^{-1}$. (a) 100 $\mu$m diameter drops; (b) 1000 $\mu$m diameter drops.

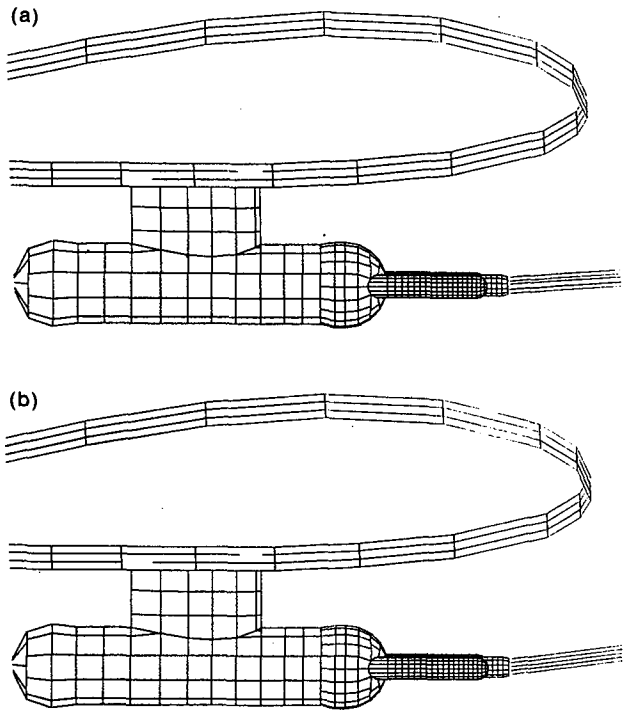


FIG. 9. Water drop flux tubes to the FSSP. Airplane angle of attack is 0°, and freestream airspeed is 49 m s$^{-1}$. (a) 100 $\mu$m diameter drops; (b) 1000 $\mu$m diameter drops.

Figures 8 and 9 show computer plots of portions of flux tubes to the wing-mounted instruments. It is clear that trajectories to or near the instruments are in no danger of intersecting the wing surface.

### b. OAP

Concentration factor and speed ratio results are shown in Figs. 10 and 11. For the isolated instrument there is little variation of concentration factor and speed ratio with either air speed or angle of attack, so that average values are plotted. The slight fall-off of concentration factor and speed ratio as drop size decreases is caused by the effect at the laser beam of flow stagnation against the forward hemisphere of the canister (Fig. 2).

To fully understand results for the wing-mounted instrument, it is necessary to consider flow conditions under the Twin Otter wing more carefully. Since at 0° angle of attack the wing is tilted (leading edge up) 2.5° relative to the freestream, there is a slight stagnation condition, with attendant slight divergence and reduction in flow speed, under the wing in the region immediately forward of the instrument (Fig. 6). This condition primarily affects drops in the intermediate size range (diameters in the approximate range 20–200 $\mu$m). However, further aft, this stagnation condition is overcome by slight convergent flow required

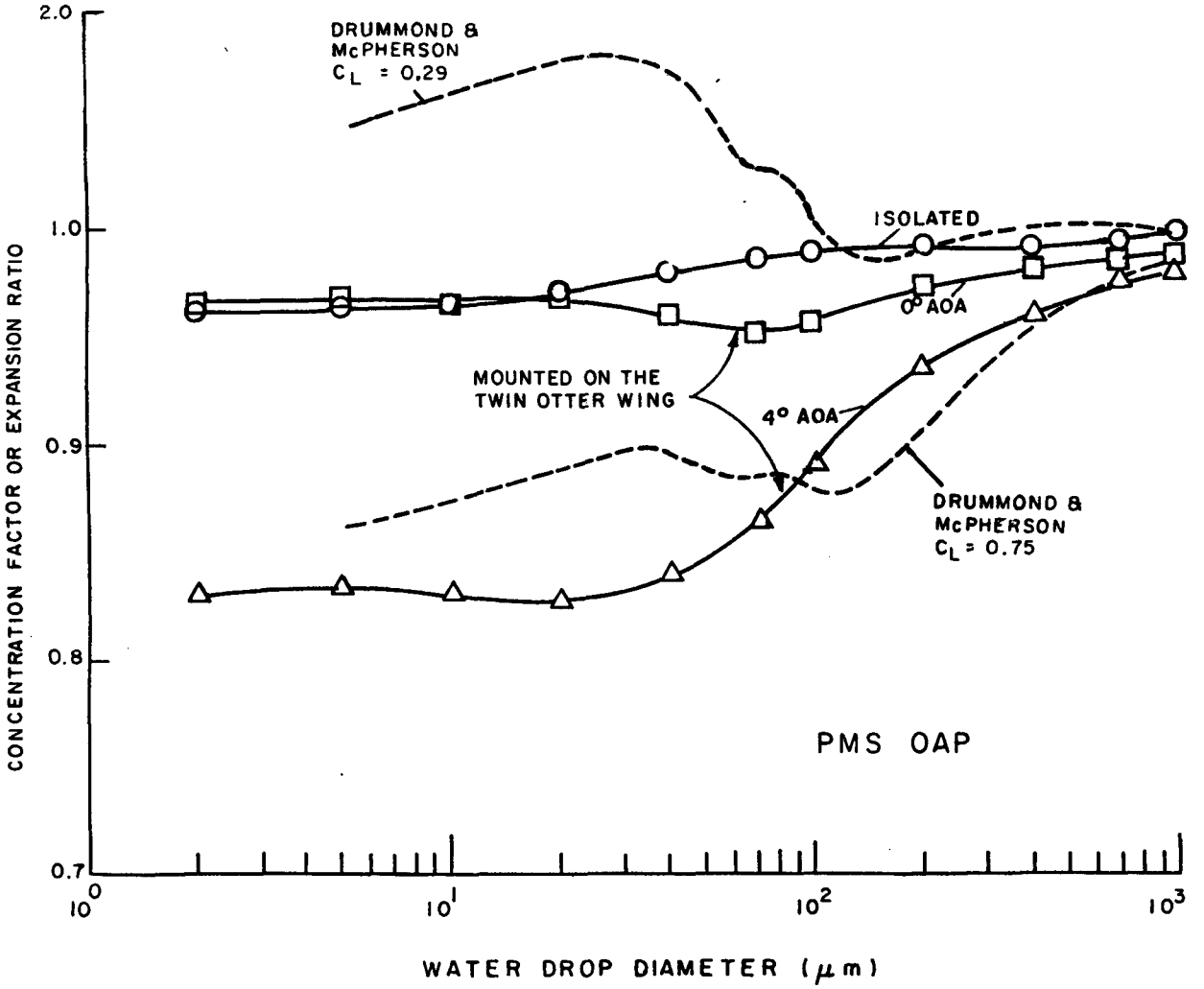


FIG. 10. Concentration factor (this study) and expansion ratio (Drummond and MacPherson 1985; see text) vs. water drop diameter for the PMS OAP. Average results are plotted for 0° and 4° angles of attack and freestream speeds of 49 and 129 m $s^{-1}$ for the isolated instrument, and for 49 and 67 m $s^{-1}$ for the wing-mounted instrument.

to negotiate the convex surface of the underside of the wing leading edge; indeed, at the location of the laser beam with the airplane at 0° angle of attack and without the instrument, air flow speed is found to be slightly greater than freestream. With the airplane at 4° angle of attack, the under-wing partial stagnation condition is, of course, more pronounced, and it prevails both forward of the instrument and at the location of the laser beam.

Flux and speed ratio results for the wing-mounted OAP are completely consistent with this picture of the flow. For the airplane at 0° angle of attack, the curves in Figs. 10 and 11 show minima at about 70 μm, which are caused by the upstream stagnation effect on the midrange size drops. As drop size decreases, results rise slightly and level off slightly below unity principally because of the stagnation effect at the laser beam caused by divergent flow about the canister. For 4° angle of attack, the fall-off of the curves with decreasing drop size is much more dramatic as well as more persistent, as expected. These results predict undermeasurement by about 17% for both flux and drop speed throughout the cloud size range when the airplane is at 4° angle of attack.

It is particularly interesting to compare Figs. 10 and 11 with Figs. 12 and 13. (In Figs. 12 and 13, concentration factor and speed ratio vs. drop diameter at the laser beam location under the Twin Otter wing are plotted but with the instrument and its mount omitted.) This comparison indicates that the instrument makes a major contribution to the distortions. At 0° angle of attack, roughly half the divergence effects for intermediate size drops and all for small drops is caused by the instrument. At 4° angle of attack, slightly less than

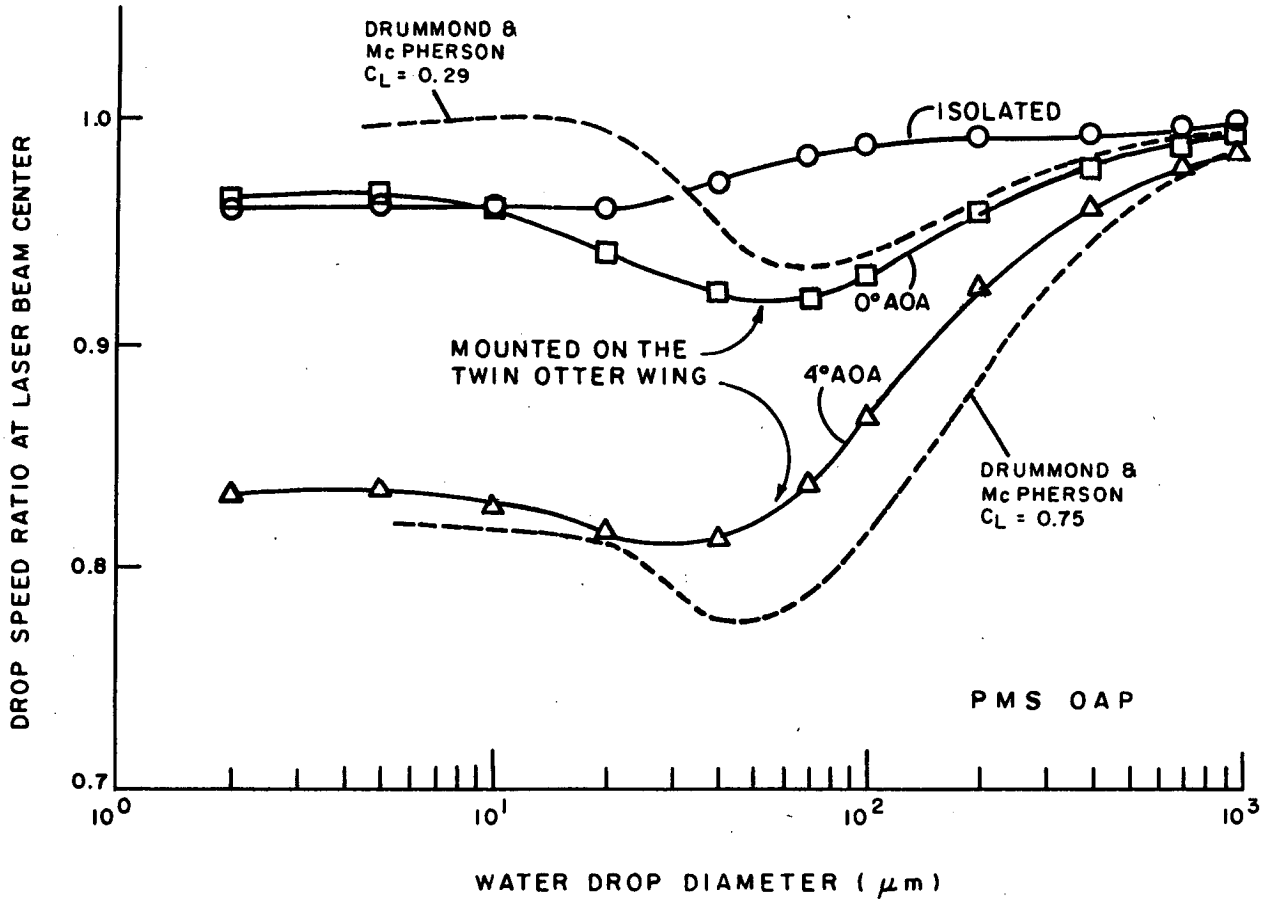


FIG. 11. Speed ratio vs. water drop diameter for the PMS OAP. Average results are plotted for 0° and 4° angles of attack and freestream speeds of 49 and 129 m $s^{-1}$ for the isolated instrument, and for 49 and 67 m $s^{-1}$ for the wing-mounted instrument. The Drummond and MacPherson (1985) curves are obtained as described in the text.

half of the effects for both intermediate and small drops are caused by the instrument.

Also plotted in Figs. 10 and 11 are the results of a similar study by Drummond and MacPherson (1985) of an OAP mounted under the wing of the Canadian National Aeronautical Establishment Twin Otter at the same location as the NASA OAP. The only difference in the Canadian instrumentation is that the mounting pylon (Fig. 5) is 2.54 cm (1″) long, while the NASA pylon is 12.7 cm (5″) long. This puts the laser beam at a distance of approximately 15 cm (6″) from the wing surface for the CNAE instrument compared with 25 cm (10″) for the NASA instrument. Drummond and MacPherson use two-dimensional Joukowski airfoil theory to calculate flow about the wing. The effects of the instrument on the flow are approximated by adding the potential function contribution for a sphere to that of the airfoil, the sphere being placed at the location of the forward canister hemisphere, while the remainder of the instrument structure is ignored. Expansion ratio (Fig. 10) is the two-dimensional analog of concentration factor.

Drummond and MacPherson express flight conditions in terms of lift coefficient or $C_L$. From observed flight data, MacPherson (1988, private communication) estimates that our 0° and 4° angles of attack correspond to lift coefficients of 0.29 and 0.75 respectively. Using these $C_L$ values, the dashed-line curves in Figs. 10 and 11 here are constructed using Figs. 12 and 13, and Eq. (17) from the Drummond and MacPherson (1985) paper. A comparison of the corresponding speed ratio curves in Fig. 11 shows remarkable agreement in spite of differences in geometries and calculation methods. The larger differences seen in Fig. 10 between concentration factor and expansion ratio, may, in part, be interpreted as an illustration of how seemingly minor differences in flow may be magnified in their effects on particle fluxes. The Drummond and MacPherson $C_L$ = 0.29 curves for both speed ratio and flux lie above our 0° curves as expected, since the Canadian instrument is approximately 10 cm closer to the wing surface than the NASA instrument, where the flow is more convergent, especially at the lower angle of attack. At the 4° angle of attack, the Drummond-MacPherson

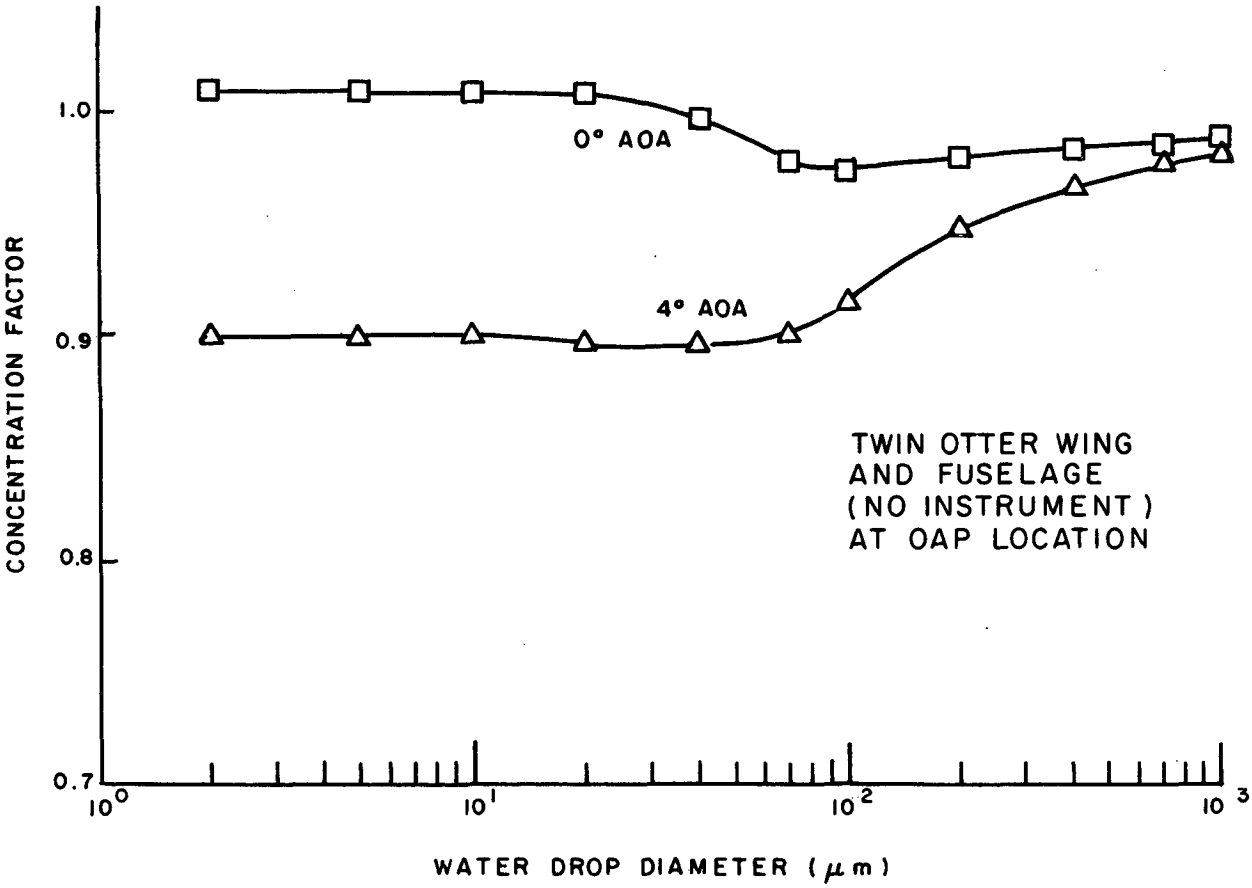


FIG. 12. Concentration factor vs. water drop diameter at the location under the Twin Otter wing of the center of the OAP laser beam, but without the instrument. Average results for freestream speeds of 49 and 67 m $s^{-1}$ are plotted.

expansion ratio curve for large drops lies below our $C_F$ curve, as is consistent with the relative positions of the speed ratio curves. However, the curves cross at about 90 $\mu$m with the consequence that the Drummond-MacPherson curve lies substantially above ours over most of the midrange of drop sizes. The reason for this is not immediately obvious, although it may partly result from additional flow stagnation caused by the instrument probe arms, which are included in our calculations but not in those of Drummond and MacPherson.

*c. FSSP*

FSSP results are plotted in Figs. 14 and 15 for 49 m $s^{-1}$ freestream air speed only. While for small drops there are persistent effects resulting from variation of freestream air speed, the maximum effect, which is for the isolated instrument, is less than 3%, which is of no practical consequence. (More complete data, including graphs for higher freestream air speeds and tabulations of results, are given in Norment 1988.) Concentration factors were calculated using flux tubes of two radii as described above. Those calculated via the coarser tubes (solid curves in Fig. 14) predict the overall collection efficiency of the measurement tube, while those calculated via the finer tubes (broken curves in Fig. 14) predict the collection efficiencies for the most important portion of the measurement volume.

For the isolated instrument, results are insensitive to angle of attack, as is also the case for the OAP. For the instrument mounted under the Twin Otter wing, there is substantial sensitivity to angle of attack, again, as is also found for the OAP. However, except for the largest drops, for which we expect little flux or speed distortion in any case, the distortions are more severe for the FSSP than for the OAP. Since differences in results at the two instrument locations without the instruments are minor[3] (compare Figs. 16 and 17 with

[3] The most pronounced differences are for the 0° angle of attack curves, which reflect differences in flow convergence under the wing at the measuring volumes of the two instruments. The OAP measuring volume is slightly closer to the wing surface, where there is slightly greater convergent flow, than is the case for the FSSP.

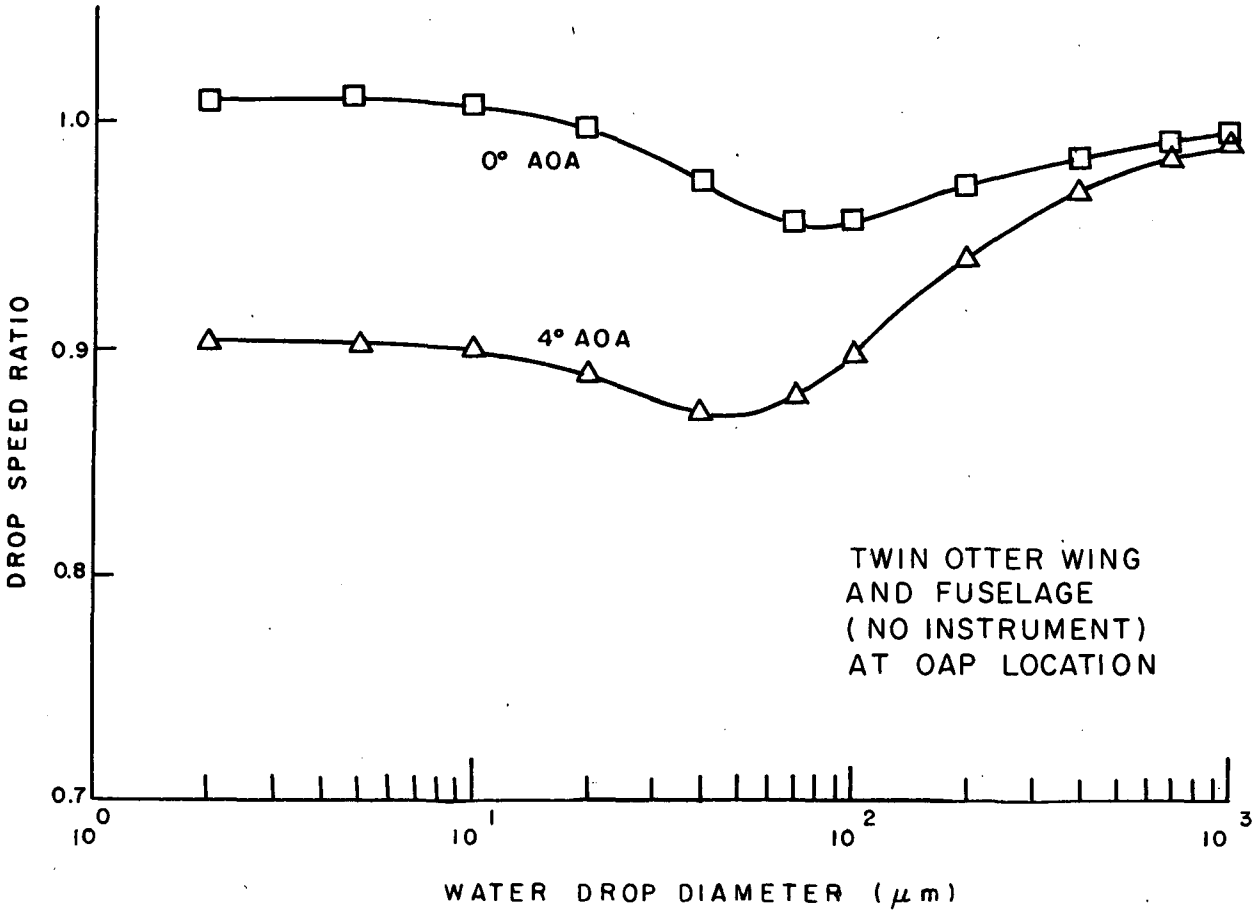


FIG. 13. Speed ratio vs. water drop diameter at the location under the Twin Otter wing of the center of the OAP laser beam, but without the instrument. Average results for freestream speeds of 49 and 67 m $s^{-1}$ are plotted.

Figs. 12 and 13), it must follow that the bulk of the differences is caused by differences in flow around and through the instruments. This conclusion is particularly evident when results for the isolated instruments are compared. Thus, we find that the presence of the instruments, and even details of their geometries and operations, cause significant flow effects. This is an important finding, since it has been common practice to assume that effects of flow perturbations caused by the instruments themselves are not significant compared with effects caused by flow about the airplane on which they are mounted.

Regardless of whether we consider solid or broken curves in Fig. 14, we predict significant flux distortions for droplets in the cloud size range (diameters < 50 μm). Quantitatively, these results predict flux measurement errors by the Twin Otter FSSP on the order of 12%–25% caused by flow effects alone. Reasons for this are clear. Not only does the structure of the support arm-measurement tube combination present a considerable obstacle to flow, but the air and drops must enter and traverse the measurement tube.

As discussed above, air flux through the measurement tube is reduced 8% relative to freestream for the isolated instrument, while for the wing-mounted instrument, flux into the tube center is reduced by 10% and 23% relative to freestream for 0° and 4° angles of attack (see Table 4). The results in Figs. 14 and 15 are consistent with this. As noted previously, both concentration factor and speed ratio approach air flux (i.e., air speed) values as particle size approaches zero, whereas for large, massive particles, both concentration factor and speed ratio are essentially unity. Thus, concentration factors calculated from the finer flux tubes (broken curves in Fig. 14) and speed ratios (Fig. 15) are expected to approach values of 92% (isolated instrument), 90% (wing mounted, 0° angle of attack) and 77% (wing mounted, 4° angle of attack) for the smallest droplets. (Concentration factor curves calculated from the coarser flux tubes are expected to approach lower minima for small droplets because the coarser tubes are more affected by diverging flow about the orifice edges and other obstructing structures.) These expectations are essentially realized for speed

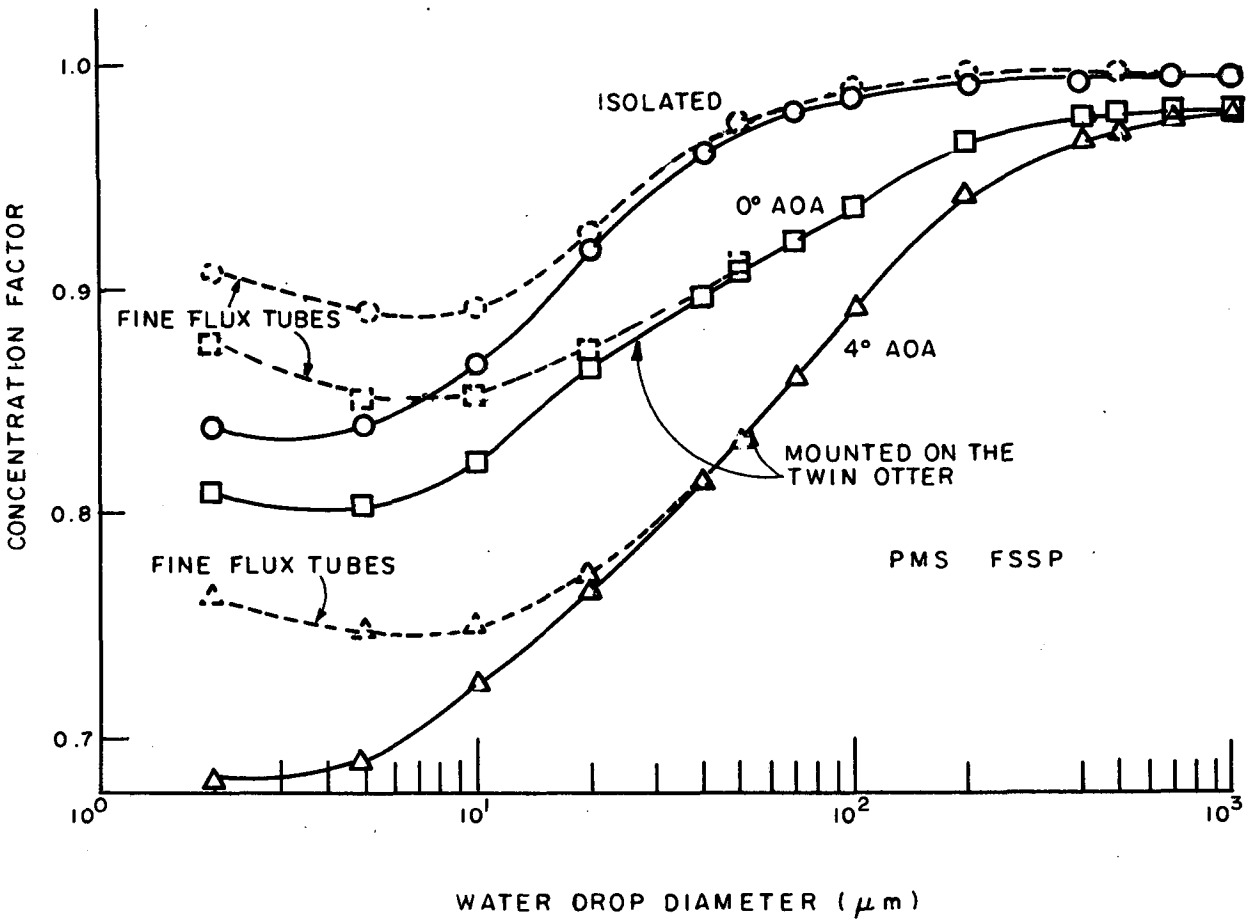


FIG. 14. Concentration factor vs. water drop diameter for the PMS FSSP with freestream speed of 49 m $s^{-1}$. Average results for 0° and 4° angles of attack are plotted for the isolated instrument. Flux tube radii at the measurement tube orifice are slightly less than the orifice radius for the solid curves and half of the orifice radius for the broken curves.

ratios in all cases, and for concentration factors at 4° angle of attack for the wing-mounted FSSP. On the other hand, concentration factor curves for the isolated and wing-mounted FSSP at 0° angle of attack pass through minima at about 7 μm droplet diameter and then rise fairly sharply toward the small-drop limit. It is surprising for droplets as small as 2 μm that concentration factors remain considerably below the limits, although the curves indicate that the limits would be reached by still smaller droplets.

## 7. Conclusions

### *a. Isolated instruments*

For the OAP we predict insensitivity of both concentration factor and speed ratio to both angle of attack and freestream air speed. The only distortions are slight slowing and slight flux divergence for small droplets caused by an upstream effect, at the location of the laser beam, of flow stagnation against the forward hemispherical end of the canister. These distortions are of little practical importance.

The FSSP presents greater obstruction to flow than the OAP owing to the presence of the measurement tube and to the large size of its support arms; in addition, it requires that both air and drops traverse the interior of the measurement tube. Again, no angle of attack effects are found. Persistent effects caused by variation of freestream air speed found in the diameter range from about 5 to 50 μm for both concentration factor and drop speed ratio, though these effects are of no practical significance. Both concentration factor and speed ratio approach limits of about 0.9 for small drops, which is consistent with our estimate of air flux through the measurement tube. The results predict that flux measurements of droplets in a size range typically found in clouds (diameters < 20 μm) would be too low by about 10%. Measurements of rain-size drops are little affected by the flow.

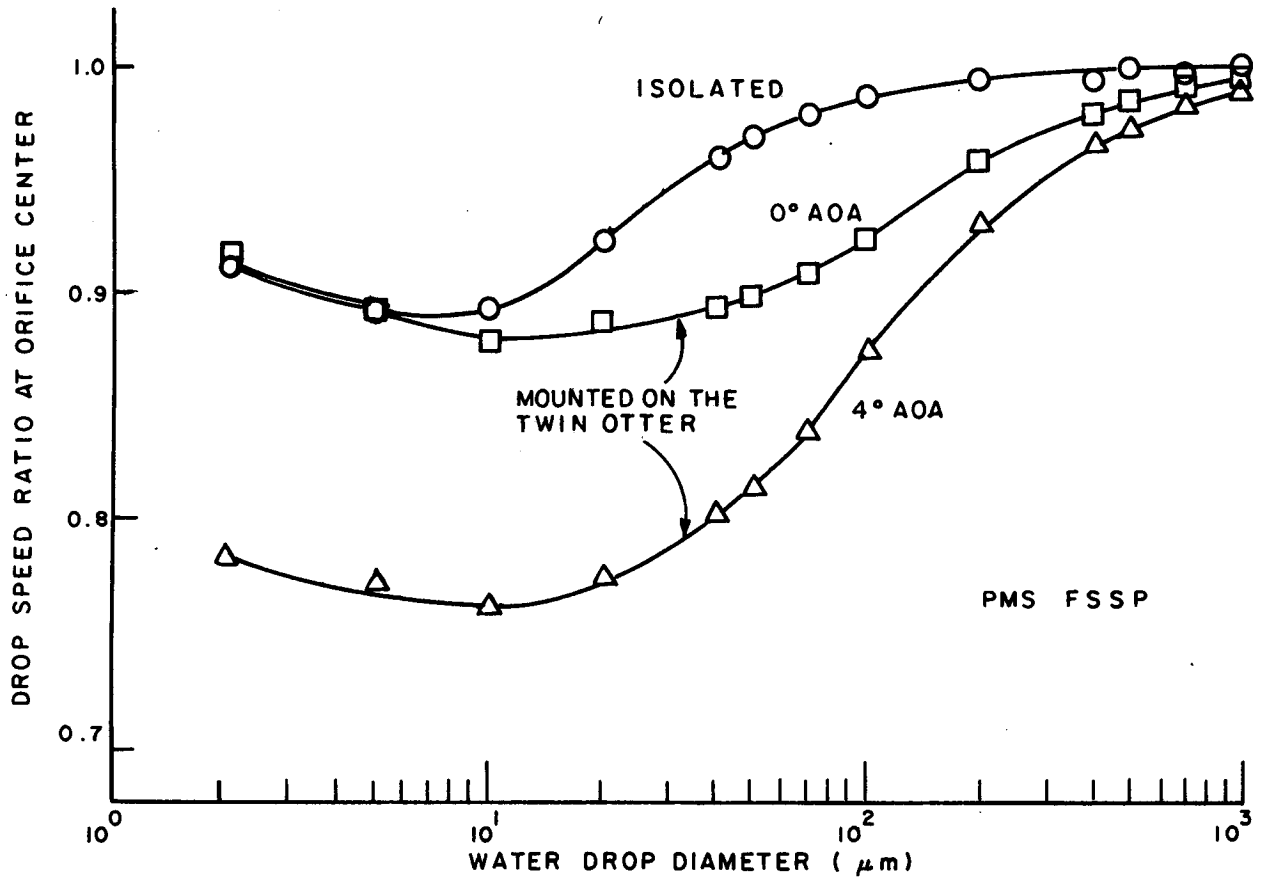


FIG. 15. Speed ratio vs. water drop diameter for the PMS FSSP with freestream speed of 49 m $s^{-1}$. Average results for 0° and 4° angles of attack are plotted for the isolated instrument.

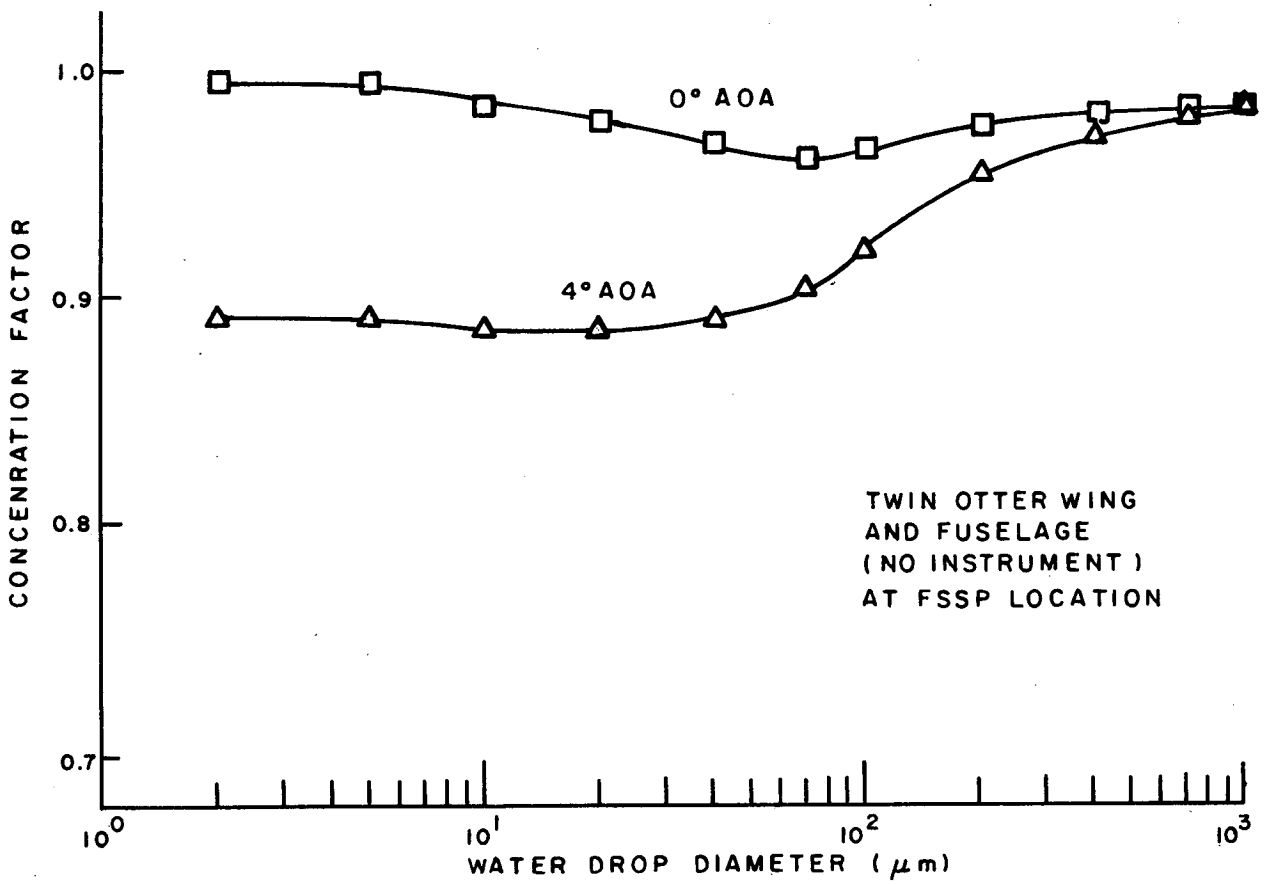


FIG. 16. Concentration factor vs. water drop diameter at the location under the Twin Otter wing of the center point of the FSSP measurement tube orifice, but without the instrument. Average results for freestream speeds of 49 and 67 m $s^{-1}$ are plotted.

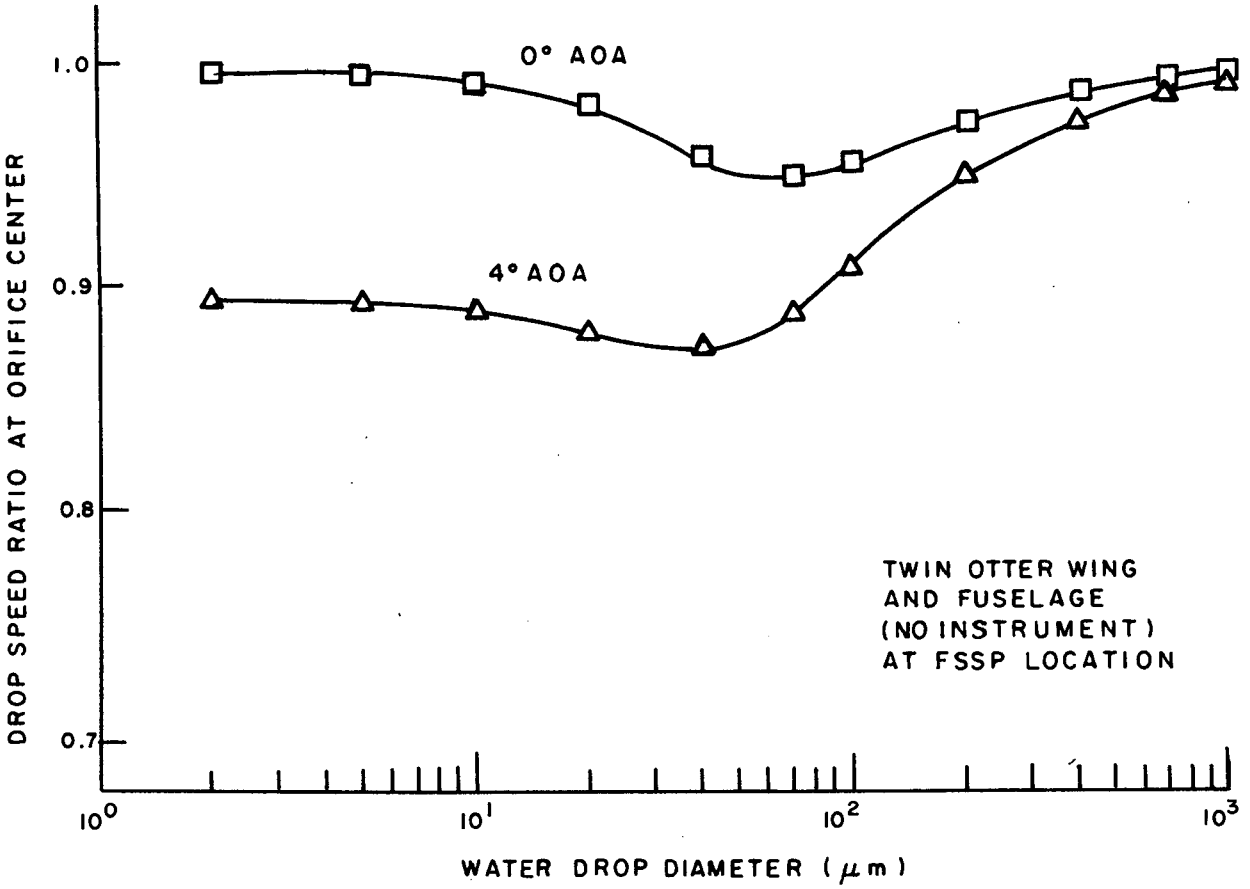


FIG. 17. Speed ratio vs. water drop diameter at the location under the Twin Otter wing of the center of the FSSP measurement tube intake orifice, but without the instrument. Average results for freestream speeds of 49 and 67 m $s^{-1}$ are plotted.

*b. Wing-mounted instruments*

For the OAP, results are insensitive to freestream air speed, but substantial angle of attack effects are found. At 0° angle of attack, distortions of drop flux and speed are small enough to be of little practical consequence. However, at 4° angle of attack, significant decreases in both drop speed and flux are found for droplets with diameters less than about 150 μm. Much of this is caused by partial flow stagnation against the under side of the uptilted wing. Minima in curves of concentration factor and speed ratio vs. drop diameter are 0.83 and 0.81 respectively. The concentration factor curve remains constant at its minimum value for drop diameters less than 20 μm. The speed ratio curve reaches its minimum at about 30 μm and then rises to stabilize at about 0.83 for smaller drops. Undermeasurement by about 17% of both flux and transit speed through the laser beam is predicted for all cloud-size droplets when the airplane is at 4° angle of attack. These results agree satisfactorily with two-dimensional calculation results by Drummond and MacPherson (1985).

For the FSSP we again find very significant angle of attack effects on both flux and speed ratio. In all cases, the distortions are substantially greater than are found for the OAP. Air speed effects are persistent for small drops but are of no practical significance. For small droplets, in the cloud droplet size range, we predict undermeasurement of both flux and speed of from 10% to 13% at 0° angle of attack, to about 24% at 4° angle of attack. (We repeat that these errors are caused by flow effects alone.) Measurements of rain-size drops are little affected by the flow.

A comparison of results calculated with and without the instruments mounted under the Twin Otter wing show that roughly half of the flux and speed distortions are caused by the presence of the instruments themselves. This finding is quite significant because it has been common practice to ignore the presence of the instruments on the assumption that flow perturbation effects caused by them are not likely to be significant compared with those caused by the aircraft on which they are mounted.

*Acknowledgments.* This work could not have been done without the support and assistance of Dr. Robert

J. Shaw of NASA Lewis Research Center and Ms. Angela Quealy of Sverdrup Technology, Inc. The work was partly funded by a contract with NASA Lewis Research Center.

## REFERENCES

Davies, C. N., 1945: Definitive equations for the fluid resistance of spheres. *Proc. Phys. Soc. London,* **57,** 259–270.

Drummond, A. M., 1984: Aircraft flow effects on cloud droplet images and concentrations. NAE-AN-21, NRC No. 23508.

——, and J. I. MacPherson, 1984: Theoretical and measured airflow about the Twin Otter wing. NAE-AN-19, NRC No. 33184.

——, and ——, 1985: Aircraft flow effects on cloud drop images and concentrations measured by the NAE Twin Otter. *J. Atmos. and Oceanic Tech.,* **2,** 633–643.

Friedman, D. M., 1974: Improved solution for potential flow about arbitrary axisymmetric bodies by use of a higher-order surface source method. Part II: User's manual for computer program. McDonnell Douglas Rep. J6627-02, NASA CR 134695 [NTIS N74-33792].

Gunn, R., and G. D. Kinser, 1949: The terminal velocity of fall for water drops in stagnant air. *J. Meteor.,* **6,** 243–248.

Hess, J. L., 1972: Calculation of potential flow about arbitrary three-dimensional lifting bodies, McDonnell Douglas Rep. J5679-01 [NTIS AD-755 480].

——, and R. P. Martin, 1974: Improved solution for potential flow about arbitrary axisymmetric bodies by use of a higher-order surface source method. Part I: Theory and results. McDonnell Douglas Rep. J6627-01, NASA CR 134694. [NTIS N74-33791].

Knollenberg, R. G., 1970: The optical array: An alternative to scattering or extinction for airborne particle size determination. *J. Appl. Meteor.,* **9,** 86–103.

——, 1976: Three new instruments for cloud physics measurements: The 2-D Spectrometer, the Forward Scattering Probe, and the Active Scattering Aerosol Spectrometer. *Preprints, International Conference on Cloud Physics,* Boulder, Amer. Meteor. Soc., 554–561.

NOAA and NASA, 1976: *U.S. Standard Atmosphere,* NOAA-S/T76-1562.

Norment, H. G., 1976: Effects of airplane flowfields on hydrometeor concentration measurements. *Preprints, International Conference on Cloud Physics,* Boulder, Amer. Meteor. Soc., 591–596.

——, 1985a: Three-dimensional airflow and hydrometeor trajectory calculation with applications. 23rd Aerospace Meeting, Reno, AIAA Paper AIAA-85-0412.

——, 1985b: Calculation of water drop trajectories to and about arbitrary three-dimensional lifting bodies in potential airflow. NASA Contractor Rep. 3935 [NTIS N87-11694/3/GAR].

——, 1988: Three-dimensional trajectory analyses of two drop sizing instruments: PMS OAP and PMS FSSP. NASA CR 4113, DOT/FAA/CT-87130.

——, and R. G. Zalosh, 1974: Effects of airplane flowfields on hydrometeor concentration measurements. AFCRL-TR-0602 [NTIS AD-A006 690].

Shaw, R. J., R. F. Ide, H. G. Norment and A. Quealy, 1986: The use of a three-dimensional water drop trajectory analysis to aid in interpreting icing cloud data. 24th Aerospace Meeting, Reno, AIAA, Paper AIAA-86-0405.